



Synthesis and properties of group 9 metal complexes bearing a β -ketophosphenato ligand

Teruyuki Matsumoto, Takahiro Sasamori, Nobuhiro Takeda¹, Norihiro Tokitoh*

Institute for Chemical Research, Kyoto University, Gokasho, Uji, Kyoto 611-0011, Japan

ARTICLE INFO

Article history:

Received 2 October 2009
Received in revised form 17 October 2009
Accepted 20 October 2009
Available online 24 October 2009

Keywords:

Monovalent bidentate ligand
 β -Ketophosphenato ligand
Low-coordinated phosphorus ligand
Rhodium complex
Iridium complex

ABSTRACT

A novel β -ketophosphenato ligand bearing a bulky substituent, Tbt(2,4,6-tris[bis(trimethylsilyl)methyl]phenyl), on the phosphorus atom was newly designed and synthesized as a heavier congener of a β -ketoiminato ligand. Rhodium and iridium complexes bearing this new β -ketophosphenato ligand have been synthesized and fully characterized by spectroscopic and elemental analyses together with X-ray crystallographic analyses. The results of NMR spectroscopic studies and the X-ray structural analyses suggested that the β -ketophosphenato ligand has unique electronic features due to the low-coordinated phosphorus atom. Comparison of properties between rhodium β -ketophosphenates **2a,b** and rhodium β -ketoiminato **7** revealed the character of the β -ketophosphenato ligand, where the trans influence of the phosphorus atom should be stronger than the nitrogen atom of the β -ketoiminato ligand.

© 2009 Elsevier B.V. All rights reserved.

1. Introduction

The coordination chemistry of β -diketiminato and β -ketoiminato ligands has attracted much interest especially in the fields of olefin polymerization based on late transition metals [1,2]. The principal advantage of β -diketiminato and β -ketoiminato ligands can be summarized as follows: (i) facile preparation, (ii) strong coordination ability to the transition metal center as a monovalent and bidentate ligand, and (iii) steric effect afforded by the bulky substituent on the nitrogen atom(s). Particularly, a β -ketoiminato ligand features unique properties due to its moderate coordination ability toward a transition metal center lying between β -diketiminato (stronger) and Schiff-base (weaker) ligands to the same metal center (Scheme 1) and its unsymmetrical *trans* effect based on the difference of the coordinating atoms (nitrogen and oxygen) [2].

On the other hand, P,O-chelating monoanionic ligands, phosphinoenolate ligands, have been well-studied [3]. Phosphinoenolates ligands have sp^3 -phosphorus atom and enolate moiety for coordination sites that form five-membered ring chelated with transition metals. Phosphinoenolate metal complexes have been found to have wide applications for catalytic reactions especially in telomerization of CO₂ and butadiene, polymerization of ethylene and

transfer dehydrogenation of alkanes. Their chemical modifications are so easy that ligands are fine-tunable for every catalytic reaction.

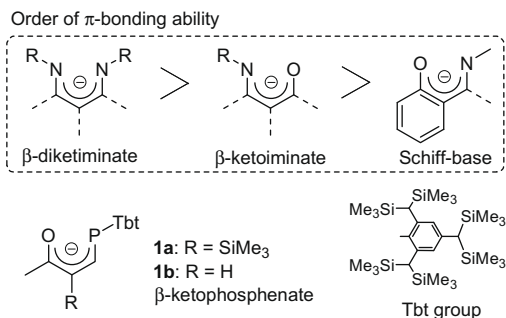
In addition, the coordination chemistry of phosphalkenes has drawn a great deal of recent attention due to their unique electronic properties of the C=P double-bond, whose characteristic low-lying π^* orbital makes it possible to work as a good π acceptor toward a transition metal center [4]. However, it is difficult to isolate and handle compounds bearing a P=C double-bond. Kinetic stabilization afforded by a bulky substituent has been proven to be very effective for the construction of doubly bonded systems containing (a) heavier atom(s) [5]. We have also reported the synthesis of a series of doubly bonded systems between heavier group 15 elements, ArE = EAr (E = P, Sb, Bi), as stable compounds by taking advantage of our original steric protection groups, 2,4,6-tris[bis(trimethylsilyl)methyl]phenyl(Tbt) and 2,6-bis[bis(trimethylsilyl)methyl]-4-[tris(trimethylsilyl)methyl]phenyl(Bbt) groups, and revealed their unique properties [6,7].

Recently, we have reported the application of Tbt group toward the synthesis of an extremely bulky β -diketiminato ligand and their complexation with group 4 metals [8]. During the course of our investigations on the low-coordinated species of heavier group 15 elements and the extremely bulky β -diketiminato ligand, we designed novel β -ketophosphenato ligands **1** [9], which have both features of β -ketoiminato and low-coordinated phosphorus ligands [10]. We have preliminarily reported the synthesis and properties of β -ketophosphenato complexes as touchstones for the elucidation of the properties of β -ketophosphenato ligands **1a,b** [11] and

* Corresponding author. Fax: +81 774 38 3209.

E-mail address: tokitoh@boc.kuicr.kyoto-u.ac.jp (N. Tokitoh).

¹ Present address: Department of Chemistry and Chemical Biology and International Education and Research Center for Silicon Science (Silicon Center), Graduate School of Engineering, Gunma University, Kiryu, Gunma 376-8515, Japan.



Scheme 1. Typical types of monovalent bidentate ligands.

the synthesis and property of a P,N-chelating ligand as phosphorus analogues of a Schiff-base type ligand [12]. We report here the synthesis and detailed properties of the rhodium and iridium complexes bearing a β -ketophosphenato ligand.

2. Results and discussion

2.1. Synthesis of ligand precursors **3a,b**

Ligand precursors **3a,b** were synthesized as shown in Scheme 2. Tbt-substituted silylphosphine was synthesized in a good yield by modifying the reported method [13], i.e., the treatment of TbtPH(Li) with trimethylsilyl chloride. Since Tbt-substituted silylphosphine was highly reactive toward water and oxygen, it was used for the next reaction without further purification. When the Tbt-substituted silylphosphine was treated with 3-butyn-2-one, **3a** was obtained via silylphosphination toward carbonyl-activated carbon–carbon triple bond [14]. It was found that the silylphosphination reaction proceeded in *syn*-fashion. α -Carbonyl-substituted trimethylsilyl group of **3a** was removed with potassium fluoride to afford **3b**. While **3a** is inert toward water and oxygen, **3b** gradually decomposed in the air to afford oxidized compounds. *E/Z* isomerization of **3a** or **3b** was not observed under ambient conditions.

The molecular structure of **3a** is shown in Fig. 1. C1–C2 and C3–O1 bond lengths are 1.345(4) and 1.222(4) Å, respectively, which are in the range of typical C=C and C=O double-bond lengths. P1–C1 and C2–C3 bond lengths are 1.808(3) and 1.501(4) Å, respectively, which are in the range of typical C–C single-bond lengths. The NMR spectroscopic properties of precursors **3a,b** have also been revealed. The ³¹P NMR spectra of **3a,b** showed signals at the same value, –79 ppm, which is a typical chemical shift for secondary phosphines. In the ¹H NMR spectra of **3b**, the coupling constant between α -carbonyl methine proton and TbtPH-substituted methine proton is 17 Hz, supporting the structure of **3b**.

2.2. Synthesis of lithium β -ketophosphenate **4a**, rhodium β -ketophosphenates **2a,b** and iridium β -ketophosphenate **8b**

Deprotonation reaction of **3a** with LDA in THF afforded lithium β -ketophosphenate [**4a**·(OEt₂)₂], which was reasonably characterized by the spectroscopic and X-ray crystallographic analyses. It was found that the C=C moiety of **3a** rotated to form the cyclic structure with the central lithium atom coordinated by the P and

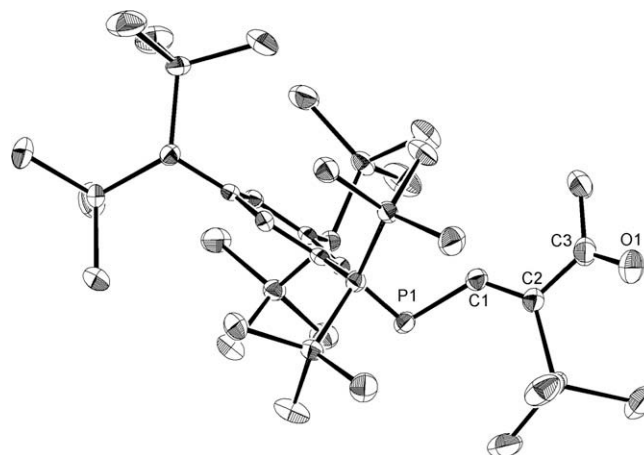


Fig. 1. ORTEP drawing of **3a** with thermal ellipsoid plots (50% probability). The hydrogen atoms are omitted for clarity.

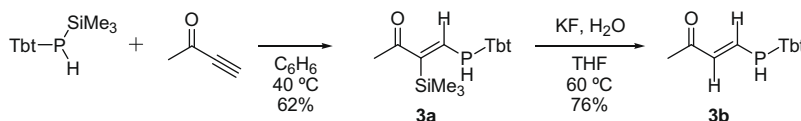
O atoms through the lithiation. The reaction of [**4a**·(OEt₂)₂] with [RhCl(cod)]₂ at room temperature in THF resulted in the formation of rhodium β -ketophosphenate **2a** in 98% yield. In contrast to the case of lithiation of **3a**, the reaction of **3b** with LDA under the same conditions afforded a complicated mixture as judged by the ¹H and ³¹P NMR spectra. Although the purification and identification of the resulting products failed, the addition of [RhCl(cod)]₂ to the reaction mixture *in situ* gave stable rhodium β -ketophosphenate **2b** in 26% yield (from **3b**) (Scheme 3).

Since it is important to evaluate the properties of β -ketophosphenato ligand as compared with those of β -ketoiminato ligands, rhodium β -ketoiminato **7** was synthesized by the reaction of [RhCl(cod)]₂ with the corresponding lithium β -ketoiminato **6**, which was prepared from β -enaminoketone **5** [15] and *n*-butyl lithium (Scheme 4).

The reaction of [**4a**·(OEt₂)₂] with [IrCl(cod)]₂ in THF resulted in the formation of iridium β -ketophosphenate **8b** bearing ligand **1b** in 94% yield as shown in Scheme 5. In this reaction, no formation of **8a** bearing ligand **1a** was observed. Unexpectedly, the SiMe₃ group of [**4a**·(OEt₂)₂] was lost via the complexation reaction, and the fate of SiMe₃ group is unclear at present.

2.3. Structural properties of lithium β -ketophosphenate **4a**, rhodium β -ketophosphenates **2a,b**, and iridium β -ketophosphenate **8b**

The structure of lithium complex **4a** was revealed by the X-ray crystallographic analysis (Fig. 3). Since there is no notable difference between the two crystallographically independent molecules in the unit cell, one of them was shown in Fig. 2. The lithium β -ketophosphenate exhibits a dimeric structure. The ligand backbone P1–C1–C2–C3–O1 showed planar structure and the lithium atom was out of the plane. In the P1–C1–C2–C3–O1 skeleton, the every bond length was medium values between those of the corresponding single and double-bonds, suggesting their delocalized π -electrons. The NMR spectroscopic properties of lithium β -ketophosphenate **4a** have also been revealed. The ³¹P NMR spectra of **4a** showed a signal in a relatively low field (162 ppm) which should indicate the *sp*²-hybridization of the phosphorus atom.



Scheme 2. Synthesis of precursors **3a, 3b**.

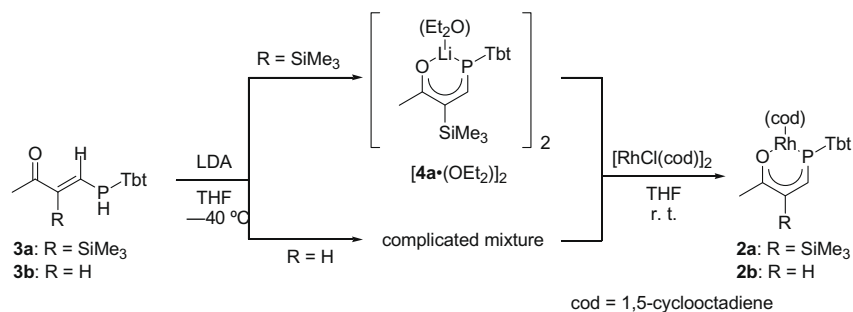
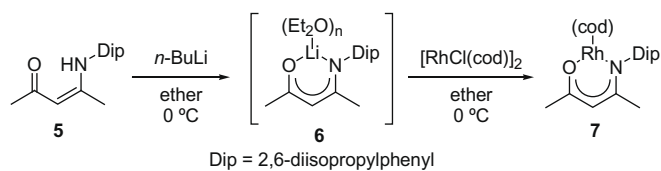
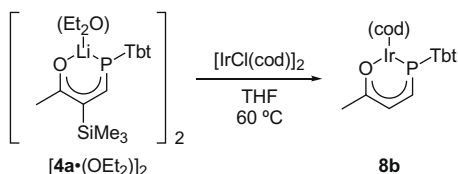
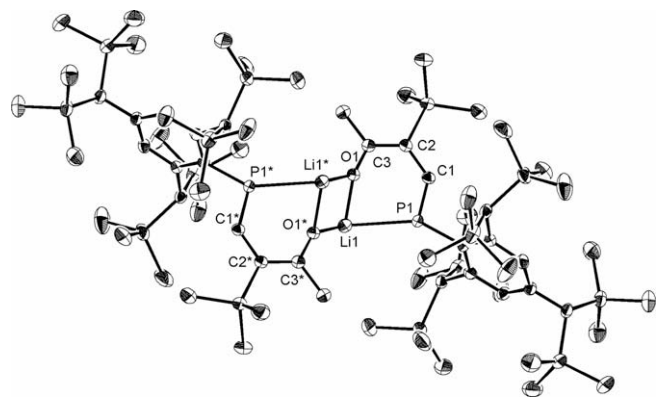
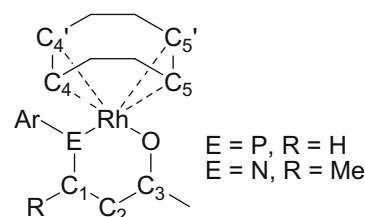
Scheme 3. Synthesis of rhodium β -ketophosphenate **2a,b**.Scheme 4. Synthesis of rhodium β -ketoiminate **7**.Scheme 5. Synthesis of iridium β -ketophosphenate **8b**.

Fig. 2. Molecular structure of the lithium β -ketophosphenate $[4a(OEt_2)_2]_2$ (0.5-hexane) (50% probability). Hydrogen atoms, hexane and diethylether were omitted for clarity. Selected bond lengths (Å): Li1–P1, 2.613(5); Li1–O1, (3); P1–C1, 1.711(3); C1–C2, 1.432(4); C2–C3 1.400(4); C3–O1, 1.297(4).

Structures of rhodium complexes **2a,b** and **7** were revealed by the X-ray crystallographic analyses (Fig. 3), and the observed structural parameters were summarized in Table 1. The phosphorus atoms of **2a** and **2b** were found to exhibit an sp^2 -hybridization on the basis of the almost planar geometry (the sum of the angles around the P atom is 359.6°). In addition, it was found that both **2a,b** and **7** showed an almost planar structure for the central six-membered ring moiety, $[-Rh-O-C-C-C-E-]$ ($E = N$ and P), where the every bond length of the central hexagonal ring was medium values between those of the corresponding single and double-bonds, suggesting their delocalized π -electrons. It should be noted that the two Rh–(cod) distances of **2a,b** were apparently different from each other, that is, the bond lengths of Rh–C4 and Rh–C4' were shorter than those of Rh–C5 and Rh–C5', though those of **7**

Table 1

Observed and calculated structural parameters for **2b**, **2b'**, **7** and **7'**. (Dmp = 2,6-dimethylphenyl).



Bond lengths (Å)	Observed		Calculated ^a		
	2b E = P Ar = Tbt	7 E = N Ar = Dip	2b' E = P Ar = Dmp	2b E = P Ar = Tbt	7' E = N Ar = Dmp
Rh–E	2.2404(8)	2.098(1)	2.3	2.332	2.136
E–C ₁	1.698(3)	1.325(2)	1.723	1.708	1.331
C ₁ –C ₂	1.396(5)	1.419(3)	1.398	1.405	1.416
C ₂ –C ₃	1.387(5)	1.372(3)	1.409	1.398	1.393
C ₃ –O ₁	1.278(4)	1.289(2)	1.28	1.286	1.281
O ₁ –Rh	2.043(2)	2.040(1)	2.095	2.089	2.064
Rh–C ₄	2.108(3)	2.116(2)	2.152	2.146	2.167
Rh–C ₄ '	2.119(4)	2.140(2)	2.171	2.174	2.191
Rh–C ₅	2.195(4)	2.152(2)	2.263	2.252	2.201
Rh–C ₅ '	2.173(4)	2.125(2)	2.242	2.214	2.174

^a Optimized at B3LYP/6-31G(d) (6-31G(3d) for Si, P; lan12DZ for Rh).

were similar to each other. These structural features suggested the stronger *trans* influence of the phosphorus moiety of β -ketophosphenato ligand **1b** as compared with its oxygen moiety in contrast to almost equal degree of *trans* influence of the both sides of N and O in **7**. Such unique unsymmetrical electronic feature of β -ketophosphenato ligand **1b** should reflect the high σ -donating ability due to the electropositive phosphorus atom and the low-lying π^* orbital of sp^2 -hybridized phosphorus atom making the back donation from the rhodium stronger.

Theoretical calculations have been performed for the model molecules bearing a less hindered substituent (Dmp; 2,6-dimethylphenyl) instead of a Tbt or Dip group, i.e., rhodium β -ketophosphenate **2b'** and rhodium β -ketoiminate **7'**, optimized at B3LYP/6-31G(d) (6-31G(3d) for Si, P; lan12DZ for Rh). The optimized structural parameters of **7'** were similar to those observed for **7**, indicating the relatively bulky Dip group less affected the structure of the rhodium β -ketoiminate skeleton. However, the optimized structure of **2b'** showed a bent structure for the central six-membered ring moiety in contrast to the observed planar structure of **2b**. Although the C–C and C–O bonds of **2b'** were found to be highly conjugated as judged by their bond lengths, the phosphorus atom showed the pyramidal geometry (the sum of the angles around the

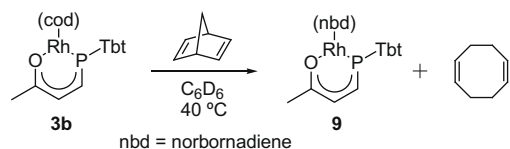
P atom is 347.1°), which is indicative of its sp^3 -hybridization. Therefore, it can be concluded that the extremely bulky Tbt group plays two important roles as follows: (i) kinetic stabilization for the reactive sp^2 -phosphorus center and (ii) steric effect of the upright geometry of two $\text{CH}(\text{SiMe}_3)_2$ moieties at *ortho* positions for keeping the planar structure of the β -ketophosphenato ligand with sp^2 -hybridized phosphorus atom and preventing the phosphorus atom from having a pyramidal structure of sp^3 -character [16]. Actually, the theoretically optimized structure of the real molecule **2b** showed the structural parameters similar to those experimentally observed with the planar skeleton of the central six-membered ring (the sum of angles around the P atom is 359.8°).

The NMR spectroscopic properties of rhodium β -ketophosphenates **2a,b** have also been revealed. The ^{31}P NMR spectra of **2a,b** showed doublet signals in a relatively low-field region, 129 ($^1J_{\text{PRh}} = 174$ Hz) and 120 ($^1J_{\text{PRh}} = 175$ Hz) ppm, respectively, which are characteristic of sp^2 -hybridized phosphorus atoms. The observed coupling constants of **2a,b**, $^1J_{\text{PRh}}$, were in the typical range of those for rhodium–phosphine or –phosphide complexes [17]. In the ^{13}C NMR spectra of **2a,b**, the chemical shifts of C_5 and C'_5 (96.5 for **2a**, 96.0 for **2b**) were observed in a lower-field region than those of C_4 and C'_4 (64.7 for **2a**, 64.4 for **2b**) (the atom numberings are according to those shown in Table 1). Thus, the NMR spectra of **2a,b** also suggested the stronger *trans* influence of the P atom than that of O atom in β -ketophosphenato ligands **1**. On the other hand, the ^{13}C NMR spectra of rhodium β -ketoiminate **7** showed the signals for its C_4 (C'_4) and C_5 (C'_5) atoms at 75.9 and 81.6 ppm, respectively, indicating the similar degree of the *trans* influence of O and N atoms in β -ketoiminate ligand.

The ^{31}P NMR spectra of **8b** showed a signal in a relatively low field (121 ppm) which should be characteristic of sp^2 -hybridized phosphorus atoms, supporting its structural features similar to those of **2b**.

2.4. Thermal ligand-exchange reaction of rhodium β -ketophosphenate **2a**

Thermal ligand-exchange reaction was examined to elucidate the difference of the electronic property between β -ketophosphenato ligand and β -ketoiminate ligand from the viewpoint of *trans* effect. The NMR studies of **3b** showed that it underwent very slow ligand-exchange reaction of the cyclooctadiene moiety in the presence of an excess amount of norbornadiene at room temperature in



Scheme 6. Ligand-exchange reaction of rhodium β -ketophosphenate.

C_6D_6 . Heating of rhodium β -ketophosphenate **2b** in the presence of norbornadiene (10 eq.) in C_6D_6 at 40°C for 5 h afforded the corresponding diene-exchanged product **8** almost quantitatively, though no diene-exchange reaction was observed in the case of heating of rhodium β -ketoiminate **7** under the same conditions. The lower barrier of the diene-exchange reaction of **3b** than that of **7** would be due to the strong *trans* effect of the P atoms of the β -ketophosphenato ligand **1b** (Scheme 6).

3. Conclusion

The first stable rhodium β -ketophosphenates **2a,b** and iridium β -ketophosphenate **9b** have been synthesized as stable compounds. Their unique properties due to the intrinsic nature of the sp^2 -hybridized P atom have been revealed based on the comparison with those of rhodium β -ketoiminate **7**. The unique unsymmetrical *trans* influence of β -ketophosphenato ligands **1** was suggested by the spectroscopic and crystallographic analyses of the corresponding complexes, where that of the phosphorus moiety should be stronger than the oxygen moieties in contrast to the similar degree of *trans* influence of the both sides of N and O atoms in a β -ketoiminate ligand. The β -ketophosphenato ligand **1a,b** should be a potentially good candidate as one of the unique ligands to make great progress in the catalytic chemistry. Further investigation of their chemical reactivity and catalytic ability of the newly obtained metal complexes is currently in progress.

4. Experimental

4.1. General experimental details

All experiments were performed under an argon atmosphere unless otherwise noted. All solvents were purified by standard

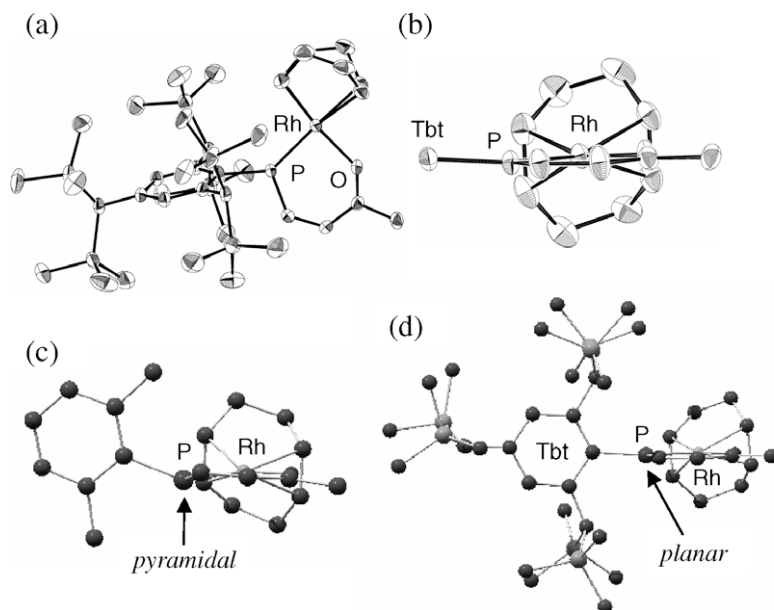


Fig. 3. (a, b) ORTEP drawing of **2b** with thermal ellipsoid plots (50% probability). Hydrogen atoms are omitted for clarity. (c) Optimized structure of **2b'**. Hydrogen atoms are omitted for clarity. (d) Optimized structure of **2b**. Hydrogen atoms are omitted for clarity.

methods and/or The Ultimate Solvent System (Glass Contour Company) [18] prior to use. ^1H NMR (400 or 300 MHz) and ^{13}C NMR (100 or 75 MHz) spectra were measured in CDCl_3 or C_6D_6 with a JEOL JNM AL-400 or JEOL JNM AL-300 spectrometer. A signal due to CHCl_3 (7.25 ppm) or $\text{C}_6\text{D}_5\text{H}$ (7.15 ppm) was used as an internal standard in ^1H NMR, and that due to CDCl_3 (77.0 ppm) or C_6D_6 (128 ppm) was used in ^{13}C NMR. Multiplicity of signals in ^{13}C NMR spectra was determined by DEPT technique. Mass spectral data were obtained on a JEOL JMS-700 spectrometer (FAB) or BRUKER micro TOF focus-Kci (ESI). GLPC (gel permeation liquid chromatography) was performed on an LC-908 or LC-918 (Japan Analytical Industry Co., Ltd.) equipped with JAIGEL 1H and 2H columns (eluent: toluene or chloroform). Preparative thin-layer chromatography (PTLC) and Wet column chromatography (WCC) were performed with Merck Kieselgel 60 PF254 and Wakogel C-200, respectively. All melting points were determined on a Yanaco micro melting point apparatus and are uncorrected. Elemental analyses were carried out at the Microanalytical Laboratory of the Institute for Chemical Research, Kyoto University. TbtPH_2 [19] and β -enaminoketone **5** [16] were prepared according to the reported procedures.

4.2. Synthesis of $\text{TbtPH}(\text{SiMe}_3)$

To a diethylether solution (10 mL) of TbtPH_2 (584 mg, 1.00 mmol) was added *n*-butyl lithium (1.51 M hexane solution, 0.79 mL, 1.2 mmol) at -78°C . After stirring at -78°C for 1 h, trimethylsilyl chloride (1.1 mL, 1.2 mmol) was added. The reaction mixture was gradually warmed up to room temperature and was stirred for 1.5 h. After removal of the solvent under reduced pressure, the crude product was dissolved in hexane and then filtered through Celite[®]. The filtrate was evaporated to afford $\text{TbtPH}(\text{SiMe}_3)$ (643 mg, 0.978 mmol, 98%). $\text{TbtPH}(\text{SiMe}_3)$: colorless crystals, m.p. $117\text{--}118^\circ\text{C}$ (decomp.); ^1H NMR (300 MHz, CDCl_3 , 298 K) δ 0.16 (s, 18H), 0.25 (s, 36H), 0.32 (d, $^3J_{\text{PH}} = 5$ Hz, 9H), 1.43 (s, 1H), 2.49 (s, 2H), 3.61 (d, $^1J_{\text{PH}} = 214$ Hz, 1H), 6.57 (s, 1H), 6.69 (s, 1H); $^{31}\text{P}\{^1\text{H}\}$ NMR (120 MHz, C_6D_6 , 298 K) δ -143 . High-resolution MS (FAB) *m/z* Calc. for $\text{C}_{30}\text{H}_{70}\text{OPSi}_7$ 657.3600. Found: 657.3586 ($[\text{M}+\text{H}]^+$). Anal. Calc. for $\text{C}_{30}\text{H}_{69}\text{OPSi}_7$: C, 54.81; H, 10.58. Found: C, 54.82; H, 10.69%.

4.3. Synthesis of precursor **3a**

To a benzene solution (30 mL) of $\text{TbtPH}(\text{SiMe}_3)$ (1.25 g, 1.90 mmol) was added a benzene solution (100 mL) of 3-butyne-2-one (446 μL , 5.70 mmol) dropwise at room temperature. The reaction mixture was stirred at 40°C for 10 h. After removal of the solvent under reduced pressure, the purification of the crude product with WCC (hexane/ether = 5/1) gave **3a** (862 mg, 1.18 mmol, 62%). **3a**: colorless crystals, m.p. $138\text{--}140^\circ\text{C}$ (decomp.); ^1H NMR (300 MHz, CDCl_3 , 298 K) δ 0.00 (s, 18H), 0.04 (s, 36H), 0.31 (s, 9H), 1.34 (s, 1H), 2.14 (s, 3H), 2.60 (s, 1H), 2.64 (s, 1H), 5.08 (dd, $^1J_{\text{PH}} = 231$ Hz, $^3J_{\text{HH}} = 7$ Hz, 1H), 6.37 (s, 1H), 6.49 (s, 1H), 7.15 (dd, $^2J_{\text{PH}} = 8$ Hz, $^3J_{\text{HH}} = 7$ Hz, 1H); $^{13}\text{C}\{^1\text{H}\}$ NMR (75 MHz, CDCl_3 , 298 K) δ 0.0 (CH_3), 0.1 (CH_3), 0.2 (CH_3), 0.3 (CH_3), 0.4 (CH_3), 0.5 (CH_3), 26.4 (CH_3), 28.7 (CH), 30.2 (CH), 121.6 (CH), 122.5 (d, $^2J_{\text{PC}} = 3$ Hz, C), 126.5 (CH), 144.6 (C), 150.2 (C), 152.4 (d, $^1J_{\text{PC}} = 14$ Hz, C), 152.9 (d, $^1J_{\text{PC}} = 26$ Hz, CH), 202.8 (d, $^2J_{\text{PC}} = 11$ Hz, C); $^{31}\text{P}\{^1\text{H}\}$ NMR (120 MHz, CDCl_3 , 298 K) δ -79 . High-resolution MS (FAB) *m/z* Calc. for $\text{C}_{34}\text{H}_{73}\text{OPSi}_7$ 724.3784. Found: 724.3763 ($[\text{M}]^+$). Anal. Calc. for $\text{C}_{34}\text{H}_{73}\text{OPSi}_7$: C, 56.29; H, 10.14. Found: C, 56.11; H, 10.25%.

4.4. Synthesis of precursor **3b**

A THF solution (30 mL) of **3a** (1.00 g, 1.38 mmol) and KF (80 mg, 1.4 mmol) was stirred at 60°C for 1 h. After removal of the solvent under reduced pressure, the crude product was dissolved in hexane and then filtered through Celite[®]. The filtrate was evaporated to afford **3b** (76% yield as judged by ^1H NMR). **3b**: colorless solid; ^1H NMR (300 MHz, C_6D_6 , 298 K) δ 0.13–0.18 (br, 54H), 1.58 (s, 1H), 1.90 (s, 3H), 2.84 (s, 2H), 4.95 (dd, $^1J_{\text{PH}} = 230$ Hz, $^3J_{\text{HH}} = 7$ Hz, 1H), 6.39 (dd, $^3J_{\text{HH}} = 7$, 17 Hz, 1H), 6.56 (s, 1H), 6.67 (s, 1H), 7.17 (ddd, $^2J_{\text{PH}} = 24$ Hz, $^3J_{\text{HH}} = 7$ Hz, 17 Hz, 1H). $^{31}\text{P}\{^1\text{H}\}$ NMR (120 MHz, CDCl_3 , 298 K) δ -79 . High-resolution MS (FAB) *m/z* Calc. for $\text{C}_{31}\text{H}_{66}\text{OPSi}_6$ 653.3467. Found: 353.3453 ($[\text{M}+\text{H}]^+$). The chemical data of **3b** could not be collected satisfactorily due to the contamination of small amount of inseparable by-products. Since it underwent gradual decomposition leading to the formation of by-products through separation procedures, the crude mixture was used in the next reaction without further purification.

4.5. Synthesis of $[\mathbf{4a}(\text{OEt}_2)]_2$

To a THF solution (5 mL) of **3a** (50 mg, 0.069 mmol) was added a THF solution (2 mL) of lithium diisopropylamide (7.7 mg, 0.072 mmol) at -40°C . After stirring for 8 h, the solvent was removed under reduced pressure. The crude product was dissolved in benzene and heated at 60°C . The solvent was removed under reduced pressure to afford $[\mathbf{4a}(\text{OEt}_2)]_2$ (51 mg, 0.063 mmol, 92%). $[\mathbf{4a}(\text{OEt}_2)]_2$: pale yellow crystals, m.p. $195\text{--}198^\circ\text{C}$ (decomp.); ^1H NMR (300 MHz, C_6D_6 , 298 K) δ 0.14–0.29 (br, 54H), 0.35 (s, 9H), 1.12 (t, $^3J_{\text{HH}} = 7$ Hz, 6H), 1.52 (s, 1H), 2.36 (s, 3H), 3.07 (s, 1H), 3.21 (s, 1H), 3.39 (q, $^3J_{\text{HH}} = 7$ Hz, 4H), 6.62 (s, 1H), 6.73 (s, 1H), 8.75 (d, $^2J_{\text{PH}} = 21$ Hz, 1H); $^{31}\text{P}\{^1\text{H}\}$ NMR (120 MHz, C_6D_6 , 298 K) δ 162. The satisfactory data for elemental analysis of $[\mathbf{4a}(\text{OEt}_2)]_2$ could not be obtained due to its incombustibility.

4.6. Synthesis of rhodium complex **2a**

To a THF solution (5 mL) of $[\mathbf{4a}(\text{OEt}_2)]_2$ (40 mg, 0.050 mmol) was added $[\text{RhCl}(\text{cod})_2]$ (12 mg, 0.025 mmol) at room temperature. The reaction mixture was stirred at room temperature for 10 h. After the solvent was removed under reduced pressure, benzene was added to the crude product. Then, the suspension was filtered through Celite[®]. After the solvent of the filtrate was removed, the residue was washed with hexane to afford rhodium complex **2a** (46 mg, 0.49 mmol, 98%). **2a**: orange crystals, m.p. $130\text{--}134^\circ\text{C}$ (decomp.); (300 MHz, C_6D_6 , 298 K) δ 0.16 (s, 18H), 0.19 (s, 18H), 0.28 (s, 18H), 0.38 (s, 9H), 1.46 (s, 1H), 1.87 (m, 2H), 2.05 (m, 2H), 2.28 (d, 3H), 2.34 (m, 2H), 2.46 (m, 2H), 3.06 (br, 1H), 3.18 (br, 1H), 4.10 (m, 2H), 5.43 (m, 2H), 6.57 (s, 1H), 6.69 (s, 1H), 8.42 (d, $^2J_{\text{PH}} = 13$ Hz, 1H); $^{13}\text{C}\{^1\text{H}\}$ NMR (75 MHz, C_6D_6 , 298 K) δ 0.6 (CH_3), 0.7 (CH_3), 1.0 (CH_3), 1.4 (CH_3), 1.6 (CH_3), 1.7 (CH_3), 1.9 (CH_3), 28.5 (CH_2), 29.9 (d, $J = 4$ Hz, CH_3), 30.1 (CH), 30.2 (CH), 32.3 (CH), 33.7 (d, $J = 4$ Hz, CH_2), 65.1 (d, $J = 14$ Hz, CH), 96.9 (dd, $J = 8, 13$ Hz, CH), 113.6 (d, $J = 6$ Hz, C), 122.5 (CH), 127.3 (CH), 145.4 (C), 151.3 (C), 164.9 (d, $J = 10$ Hz, CH), 176.7 (d, $J = 26$ Hz, C); $^{31}\text{P}\{^1\text{H}\}$ NMR (120 MHz, C_6D_6 , 298 K) δ 129 (d, $^1J_{\text{PRh}} = 174$ Hz). High-resolution MS (FAB) *m/z* Calc. for $\text{C}_{42}\text{H}_{84}\text{OPRhSi}_7$: 934.3700. Found: 934.3708 ($[\text{M}]^+$). Anal. Calc. for $\text{C}_{42}\text{H}_{84}\text{OPRhSi}_7$: C, 53.92; H, 9.05. Found: C, 53.94; H, 9.06%.

4.7. Synthesis of rhodium complex **2b**

To a THF solution (5 mL) of **3b** (50 mg, 0.069 mmol) was added a solution of lithium diisopropylamide (7.7 mg, 0.072 mmol) in THF (2 mL) at -40°C . After stirring for 8 h, the solvent was removed under reduced pressure. The residue was dissolved in THF (5 mL) and $[\text{RhCl}(\text{cod})_2]$ (17 mg, 0.035 mmol) was added. The reaction

mixture was stirred for 10 h. After the solvent was removed under reduced pressure, insoluble inorganic salts were removed by filtration through Celite® with benzene. After the solvent of the filtrate was removed, the residue was washed with hexane to afford **2b** (15 mg, 0.018 mmol, 26% from **3b**). **2b**: orange crystals, m.p. 130–131 °C (decomp.); ¹H NMR (300 MHz, C₆D₆, 298 K) δ 0.17 (s, 18H), 0.20 (s, 18H), 0.29 (br, 18H), 1.48 (s, 1H), 1.88 (m, 2H), 2.03 (m, 2H), 2.07 (d, 3H), 2.30 (m, 2H), 2.47 (m, 2H), 3.13 (s, 1H), 3.25 (br, 1H), 4.16 (m, 2H), 5.48 (m, 2H), 6.28 (dd, ³J_{HH} = 10 Hz, ³J_{PH} = 28 Hz, 1H), 6.59 (s, 1H), 6.71 (s, 1H), 8.23 (dd, ²J_{PH} = 13 Hz, ³J_{HH} = 10 Hz, 1H); ¹³C{¹H} NMR (75 MHz, C₆D₆, 298 K) δ 1.0 (CH₃) 1.4 (CH₃), 1.8 (CH₃), 28.3 (CH₂), 28.7 (d, *J* = 4 Hz, CH₃), 30.1 (CH), 30.3 (CH), 31.0 (CH), 33.4 (d, *J* = 4 Hz, CH), 64.4 (d, *J* = 14 Hz, CH), 95.7 (dd, *J* = 9, 13 Hz, CH), 107.9 (d, *J* = 4 Hz, CH), 122.5 (CH), 127.3 (CH), 145.1 (C), 151.1 (C), 160.1 (d, *J* = 18 Hz, CH), 173.0 (d, *J* = 23 Hz, C); ³¹P{¹H} NMR (120 MHz, C₆D₆, 298 K) δ 120 (d, ¹J_{PRh} = 175 Hz). High-resolution MS (FAB) *m/z* Calc. for C₃₉H₇₇OPRhSi₆ 863.3383. Found: 863.3372 ([M+H]⁺). Anal. Calc. for C₃₉H₇₆OPRhSi₆: C, 54.25; H, 8.87. Found: C, 54.26; H, 8.95%.

4.8. Synthesis of rhodium complex **7**

To a diethylether solution (20 mL) of β-enaminoketone **5** (150 mg, 0.578 mmol) was added *n*-butyl lithium (1.51 M hexane solution, 463 μL, 0.694 mmol) at 0 °C. After the reaction mixture was stirred at 0 °C for 15 min, [RhCl(cod)]₂ (142 mg, 0.289 mmol) was added. After stirring for 2 h, the solvent was removed under reduced pressure. The residue was washed with hexane to afford **7** (89 mg, 0.19 mmol, 33%). **7**: orange crystals; m.p. 167 °C (decomp.); ¹H NMR (300 MHz, C₆D₆, 298 K) δ 1.01 (d, ³J_{HH} = 7 Hz, 6H), 1.37 (d, ³J_{HH} = 7 Hz, 6H), 1.51 (s, 3H), 1.54 (m, 2H), 1.66 (m, 2H), 2.01 (s, 3H), 2.24 (m, 4H), 2.90 (m, 2H), 3.46 (sept, ³J_{HH} = 7 Hz, 2H), 4.74 (m, 2H), 5.08 (s, 1H), 7.04 (s, 3H); ¹³C{¹H} NMR (75 MHz, C₆D₆, 298 K); δ 24.0 (CH₃), 25.0 (CH₃), 25.2 (CH₃), 26.6 (CH₃), 28.1 (CH), 29.3 (CH₂), 31.7 (CH₂), 76.0 (d, ¹J_{RhC} = 14 Hz, CH), 81.6 (d, ¹J_{RhC} = 12 Hz, CH), 97.7 (CH), 124.0 (CH), 126.0 (CH), 141.2 (C), 146.1 (C), 165.2 (C), 177.7 (C). High-resolution MS (FAB) *m/z* Calc. for C₂₅H₃₆ONRh 469.1852. Found: 469.1854 ([M]⁺). Anal. Calc. for C₂₅H₃₆ONRh: C, 63.96; H, 7.73; N 2.98. Found: C, 63.91; H, 7.77; N 3.03%.

4.9. Synthesis of iridium complex **8b**

To a THF solution (25 mL) of [4a(OEt₂)₂] (172 mg, 0.10 mmol) was added [IrCl(cod)]₂ (70 mg, 0.10 mmol) at room temperature. The reaction mixture was stirred at 60 °C for 10 h. After the solvent was removed under reduced pressure, benzene was added to the crude product. Then, the suspension was filtered through Celite®. After the solvent of the filtrate was removed, the residue was washed with hexane to afford iridium complex **8b** (188 mg, 0.094 mmol, 94%). **8b**: orange crystals, m.p. 170–171 °C (decomp.); ¹H NMR (300 MHz, C₆D₆, 298 K) δ 0.17 (s, 18H), 0.18 (s, 18H), 0.29 (br, 18H), 1.49 (s, 1H), 1.86 (m, 2H), 2.01 (m, 2H), 2.06 (d, 3H), 2.23 (m, 2H), 2.38 (m, 2H), 3.07 (br, 1H), 3.19 (br, 1H), 4.02 (m, 2H), 5.20 (m, 2H), 6.44 (dd, *J* = 11, 29 Hz, 1H), 6.60 (br, 1H), 6.73 (br, 1H), 8.58 (dd, ²J_{PH} = 12 Hz, ³J_{HH} = 11 Hz, 1H); ¹³C{¹H} NMR (75 MHz, C₆D₆, 298 K) δ 0.7 (CH₃), 1.0 (CH₃), 1.4 (CH₃), 1.6 (CH₃), 1.8 (CH₃), 28.8 (CH₂), 28.9 (d, *J* = 4 Hz, CH₃), 30.2 (CH), 31.1 (CH), 32.0 (CH), 34.3 (d, *J* = 4 Hz, CH), 48.1 (s, CH), 82.3 (d, *J* = 16 Hz, CH), 109.6 (s, CH), 122.6 (CH), 126.8 (CH), 145.8 (C), 150.9 (C), 156.3 (d, *J* = 31 Hz, CH), 173.2 (d, *J* = 23 Hz, C); ³¹P{¹H} NMR (120 MHz, C₆D₆, 298 K) δ 121. High-resolution MS (FAB) Calc. for C₃₉H₇₆OSi₆P¹⁹³Ir 952.3879. Found: 952.3857 ([M]⁺).

4.10. Thermolysis of rhodium complex **2b** in the presence of norbornadiene

To a C₆D₆ solution (0.7 mL) of **2b** (6.9 mg, 8.0 μmol) in a 5φ NMR tube was added norbornadiene (8.1 μL, 0.080 mmol). The reaction mixture was degassed and sealed in the NMR tube. After heating at 40 °C for 5 h, the starting material was found to disappear as judged by the ¹H NMR spectrum. The NMR tube was opened in a glove box filled with argon gas, and the solvent and dienes were removed under reduced pressure to afford **9** (6.6 mg, 7.4 μmol, 97%). **9**: orange crystals, m.p. 211–212 °C (decomp.); ¹H NMR (300 MHz, C₆D₆, 298 K) δ 0.17 (s, 18H), 0.20 (s, 18H), 0.28 (br, 18H), 1.12 (m, 1H), 1.24 (m, 1H), 1.47 (s, 1H), 2.11 (d, 3H), 3.24 (brs, 1H), 3.37 (brs, 1H), 3.51 (brs, 2H), 4.06 (m, 2H), 4.98 (m, 2H), 6.33 (dd, ³J_{HH} = 10 Hz, ³J_{PH} = 28 Hz, 1H), 6.58 (br, 1H), 6.69 (s, 1H), 8.22 (dd, ²J = 14 Hz, ³J = 10 Hz, 1H); ¹³C{¹H} NMR (75 MHz, C₆D₆, 298 K) δ 1.5 (CH₃) 2.0 (CH₃), 2.1 (CH₃), 29.1 (d, *J* = 6 Hz, CH₃), 30.9 (CH), 31.5 (CH), 46.1 (d, *J* = 11 Hz, CH), 50.1 (s, CH), 62.9 (s, CH₂), 74.8 (dd, *J* = 7, 12 Hz, CH), 109.0 (s, CH), 122.9 (CH), 127.6 (CH), 145.5 (C), 151.0 (C), 159.7 (d, *J* = 16 Hz, CH), 174.4 (d, *J* = 22 Hz, C); ³¹P{¹H} NMR (120 MHz, C₆D₆, 298 K) δ 133 (d, ¹J_{PRh} = 197 Hz). LRMS (ESI, negative): *m/z* 831, Calc. for C₃₇H₆₉OPRhSi₆ 831 ([M–Me][−]). Since it was difficult to obtain a satisfactory result for the elemental analysis of **9** due to the extremely high air-, moisture-, and light-sensitivity, the purity was confirmed by the ¹H NMR spectrum.

5. X-ray crystallographic analysis of **2b**, **3a**, [4a(OEt₂)₂](0.5hexane) and **7**

The intensity data were collected on a RIGAKU Saturn70 CCD (system) with VariMax Mo Optic using Mo Kα radiation (λ = 0.71070 Å) for **2b**, and on a Rigaku/MSC Mercury CCD diffractometer with graphite monochromated Mo Kα radiation (λ = 0.71070 Å) for **3a**, [4a(OEt₂)₂](0.5hexane) and **7**. Single crystals suitable for X-ray analysis were obtained by slow recrystallization from THF/benzene (for **2b**), hexane (for **3a**), Et₂O/hexane (for [4a(OEt₂)₂](0.5hexane)) and benzene (for **7**). The single crystals were mounted on a glass fiber. The structures were solved by a direct method (SHELXS-97) [20] and refined by full-matrix least-squares procedures on *F*² for all reflections (SHELXL-97) [21]. All hydrogen atoms were placed using AFIX instructions, while all other atoms were refined anisotropically.

Crystal data for 2b: C₃₉H₇₆OPRhSi₆, *M* = 863.42, *T* = 103(2) K, triclinic, *P* $\bar{1}$ (no. 2), *a* = 10.0909(2) Å, *b* = 11.1677(2) Å, *c* = 22.2560(4) Å, α = 102.3125(13)°, β = 90.6913(8)°, γ = 104.4184(10)°, *V* = 2367.57(8) Å³, *Z* = 2, *D*_{calc} = 1.211 g cm^{−3}, μ = 0.573 mm^{−1}, 2θ_{max} = 51.0, 25 098 measured reflections, 8695 independent reflections (*R*_{int} = 0.0254), 637 refined parameters, GOF = 1.107, *R*₁ = 0.0396 and *wR*₂ = 0.0926 [*I* > 2σ(*I*)], *R*₁ = 0.0441 and *wR*₂ = 0.0950 [for all data], largest diff. peak and hole 0.980 and −0.710 e Å^{−3}.

Crystal data for 3a: C₃₄H₇₃OPSi₇, *M* = 725.5, *T* = 103(2) K, monoclinic, triclinic, *P* $\bar{1}$ (no. 2), *a* = 12.374(5) Å, *b* = 12.978(5) Å, *c* = 16.641(6) Å, α = 94.725(3)°, β = 104.348(3)°, γ = 116.225(3)°, *V* = 2265.2(15) Å³, *Z* = 2, *D*_{calc} = 1.064 g cm^{−3}, μ = 0.269 mm^{−1}, 2θ_{max} = 50.0, 22 030 measured reflections, 7965 independent reflections (*R*_{int} = 0.0419), 414 refined parameters, GOF = 1.090, *R*₁ = 0.0556 and *wR*₂ = 0.1237 [*I* > 2σ(*I*)], *R*₁ = 0.0721 and *wR*₂ = 0.1326 [for all data], largest difference in peak and hole 0.782 and −0.273 e Å^{−3}.

Crystal data for [4a(OEt₂)₂](0.5hexane): C₄₁H₈₉LiO₂PSi₇, *M* = 848.66, *T* = 103(2) K, monoclinic, *P*₂₁/*a* (no. 14), *a* = 25.4620(4) Å, *b* = 12.3405(2) Å, *c* = 36.7695(6) Å, β = 107.1418(7)°, *V* = 11040.3(3) Å³, *Z* = 8, *D*_{calc} = 1.021 g cm^{−3}, μ = 0.230 mm^{−1}, 2θ_{max} = 50.0, 92 054 measured reflections, 19 339 independent reflections (*R*_{int} = 0.0705), 987 refined parameters, GOF = 1.091,

$R_1 = 0.0667$ and $wR_2 = 0.1635$ [$I > 2\sigma(I)$], $R_1 = 0.0998$ and $wR_2 = 0.1896$ [for all data], largest difference in peak and hole 0.875 and $-0.671 \text{ e } \text{Å}^{-3}$.

Crystal data for 7: $\text{C}_{25}\text{H}_{36}\text{NORh}$, $M = 469.46$, $T = 103(2) \text{ K}$, monoclinic, $C2/c$ (no. 15), $a = 8.8811(2) \text{ Å}$, $b = 8.8115(2) \text{ Å}$, $c = 15.1061(3) \text{ Å}$, $\alpha = 90.6294(9)^\circ$, $\beta = 101.8877(10)^\circ$, $\gamma = 107.159(2)^\circ$, $V = 1102.04(4) \text{ Å}^3$, $Z = 2$, $D_{\text{calc}} = 1.415 \text{ g cm}^{-3}$, $\mu = 0.790 \text{ mm}^{-1}$, $2\theta_{\text{max}} = 51.0$, 9717 measured reflections, 4057 independent reflections ($R_{\text{int}} = 0.0308$), 259 refined parameters, $\text{GOF} = 1.167$, $R_1 = 0.0237$ and $wR_2 = 0.0600$ [$I > 2\sigma(I)$], $R_1 = 0.0252$ and $wR_2 = 0.0607$ [for all data], largest difference in peak and hole 0.379 and $-0.653 \text{ e } \text{Å}^{-3}$.

6. Theoretical calculations

All calculations were conducted using the GAUSSIAN 03 series of electronic structure programs [22]. The geometries were optimized with density functional theory at the B3LYP level using 6-31G(d) basis sets (for C, H, N, and O), 6-31G(3d) (for P and Si), and LanL2DZ (for Rh). It was confirmed by frequency calculations that the optimized structures have minimum energies.

7. Supplementary material

CCDC 729128, 729129, 729130 and 729131 contain the supplementary crystallographic data for **2b**, **3a**, [**4a**·(OEt₂)₂·(0.5hexane)] and **7**. These data can be obtained free of charge from The Cambridge Crystallographic Data Centre via www.ccdc.cam.ac.uk/data_request/cif.

Acknowledgements

This work was supported by Grant-in-Aid for Creative Scientific Research (No. 17GS0207), Science Research on Priority Areas (No. 20036024, “Synergy of Elements”), and the Global COE Program (“Integrated Materials Science”, Kyoto University) from the Ministry of Education, Culture, Sports, Science and Technology, Japan.

References

- [1] L. Bourget-Merle, M.F. Lappert, J.R. Severn, *Chem. Rev.* 102 (2002) 3031.
- [2] (a) X.F. Li, K. Dai, W.P. Ye, L. Pan, Y.S. Li, *Organometallics* 23 (2004) 1223; (b) D. Zhang, G.X. Jin, L.H. Weng, F.S. Wang, *Organometallics* 23 (2004) 3270; (c) B.Y. Liu, C.Y. Tian, L. Zhang, W.D. Yan, W.J. Zhang, *J. Polym. Sci. Polym. Chem.* 44 (2006) 6243.
- [3] P. Braunstein, *Chem. Rev.* 106 (2006) 134.
- [4] (a) For a review, see: P.L. Floch, *Cood. Chem. Rev.* 250 (2006) 627; (b) F. Ozawa, S. Kawagishi, T. Ishiyama, M. Yoshifuji, *Organometallics* 23 (2004) 1325.
- [5] (a) It has been demonstrated that a heavier main group element can form a stable double-bond compound when they are appropriately protected by bulky substituents. For reviews, see: L. Weber, *Chem. Rev.* 92 (1992) 1839; (b) P.P. Power, *Chem. Rev.* 99 (1999) 3463; (c) N. Tokitoh, R. Okazaki, *Coord. Chem. Rev.* 210 (2000) 251.
- [6] (a) For reviews, see: N. Tokitoh, *Acc. Chem. Res.* 37 (2004) 86; (b) R. Okazaki, N. Tokitoh, *Acc. Chem. Res.* 33 (2000) 625; (c) N. Tokitoh, R. Okazaki, *Coord. Chem. Rev.* 210 (2000) 251; (d) T. Sasamori, N. Tokitoh, *Dalton Trans.* (2008) 1395.
- [7] (a) N. Tokitoh, Y. Arai, R. Okazaki, S. Nagase, *Science* 277 (1999) 78; (b) N. Tokitoh, Y. Arai, T. Sasamori, R. Okazaki, S. Nagase, H. Uekusa, Y. Ohashi, *J. Am. Chem. Soc.* 120 (1998) 433; (c) T. Sasamori, Y. Arai, N. Takeda, R. Okazaki, Y. Furukawa, M. Kimura, S. Nagase, N. Tokitoh, *Bull. Chem. Soc. Jpn.* 75 (2005) 661; (d) T. Sasamori, N. Takeda, M. Fujio, M. Kimura, S. Nagase, N. Tokitoh, *Angew. Chem., Int. Ed.* 41 (2002) 139; (e) T. Sasamori, N. Takeda, N. Tokitoh, *Chem. Commun.* (2000) 1353; (f) T. Sasamori, N. Takeda, N. Tokitoh, *J. Phys. Org. Chem.* 16 (2003) 450; (g) N. Nagahora, T. Sasamori, N. Takeda, N. Tokitoh, *Chem. Eur. J.* 10 (2004) 6146; (h) T. Sasamori, E. Mieda, N. Nagahora, N. Takeda, N. Takagi, S. Nagase, N. Tokitoh, *Chem. Lett.* 34 (2005) 166; (i) T. Sasamori, A. Tsurusaki, N. Nagahora, K. Matsuda, Y. Kanemitsu, Y. Watanabe, Y. Furukawa, N. Tokitoh, *Chem. Lett.* 35 (2006) 1382; (j) N. Nagahora, T. Sasamori, N. Tokitoh, *Chem. Lett.* 35 (2006) 220; (k) T. Sasamori, E. Mieda, N. Nagahora, K. Sato, D. Shiomi, T. Takui, Y. Hosoi, Y. Furukawa, N. Takagi, S. Nagase, N. Tokitoh, *J. Am. Chem. Soc.* 128 (2006) 12582.
- [8] (a) H. Hamaki, N. Takeda, N. Tokitoh, *Inorg. Chem.* 46 (2007) 1795; (b) H. Hamaki, N. Takeda, T. Yamasaki, T. Sasamori, N. Tokitoh, *J. Organomet. Chem.* 692 (2007) 44; (c) H. Hamaki, N. Takeda, N. Tokitoh, *Organometallics* 25 (2006) 2457; (d) N. Takeda, H. Hamaki, N. Tokitoh, *Chem. Lett.* 33 (2004) 134.
- [9] (a) Although there has been a few reports on the theoretical calculations for a phosphorus analogue of a Schiff-base ligand from the viewpoint of catalytic activities, no example of such a unique ligand has been synthesized so far. See M.S.W. Chan, L.Q. Deng, T. Ziegler, *Organometallics* 19 (2000) 2741; (b) T.Z. Zhang, D.W. Guo, S.Y. Jie, W.H. Sun, T. Li, X.Z. Yang, *J. Polym. Sci. Polym. Chem.* 42 (2004) 4765.
- [10] The intermediacy of a β -iminophosphinato complex, which is a phosphorus analogue of a β -diketiminato complex, was proposed to be generated; see F. Basuli, J. Tomaszewski, J.C. Huffman, D.J. Mindiola, *J. Am. Chem. Soc.* 125 (2003) 10170.
- [11] T. Sasamori, T. Matsumoto, N. Tokitoh, *Organometallics* 26 (2007) 3621.
- [12] (a) N. Tokitoh, T. Matsumoto, T. Sasamori, *Heterocycles* 76 (2008) 981; (b) T. Sasamori, T. Matsumoto, N. Tokitoh, *Polyhedron*, in press, doi:10.1016/j.poly.2009.06.043.
- [13] A.M. Arif, J.E. Boggs, A.H. Cowley, J.-G. Lee, M. Pakulski, J.M. Power, *J. Am. Chem. Soc.* 108 (1986) 6083.
- [14] The 1,2-addition reaction of a silylphosphine with an activated alkyne has been reported, see M. Reisser, A. Maier, G. Maas, *Synlett* 9 (2002) 1459.
- [15] R.C. Yu, C.H. Hung, J.H. Huang, H.Y. Lee, J.T. Chen, *Inorg. Chem.* 41 (2002) 6450.
- [16] E. Urnèzius, J.K. Stephen, J.D. Protasiewicz, *Inorg. Chim. Acta* 297 (2000) 181.
- [17] (a) A.J. Naaktgeboren, R.J.M. Nolte, W. Drenth, *J. Am. Chem. Soc.* 102 (1980) 3350; (b) I. Lee, F. Dahan, A. Maisonnat, R. Poilblanc, *Organometallics* 13 (1994) 2743.
- [18] A.B. Pangborn, M.A. Giardello, R.H. Grubbs, R.K. Rosen, F.J. Timmers, *Organometallics* 15 (1996) 1518.
- [19] N. Nagahora, T. Sasamori, N. Takeda, N. Tokitoh, *Organometallics* 24 (2005) 3074.
- [20] G.M. Sheldrick, *Acta Crystallogr., Sect. A* 46 (1990) 467.
- [21] G.M. Sheldrick, SHELX-97 Program for Crystal Structure Solution and the Refinement of Crystal Structures, Institut für Anorganische Chemie der Universität Göttingen, Tammanstrasse 4, D-3400 Göttingen, Germany, 1997.
- [22] M.J. Frisch, G.W. Trucks, H.B. Schlegel, G.E. Scuseria, M.A. Robb, J.R. Cheeseman, J.A. Montgomery, T. Vreven, K.N. Kudin, J.C. Burant, J.M. Millam, S.S. Iyengar, J. Tomasi, V. Barone, B. Mennucci, M. Cossi, G. Scalmani, N. Rega, G.A. Petersson, H. Nakatsuji, M. Hada, M. Ehara, K. Toyota, R. Fukuda, J. Hasegawa, M. Ishida, T. Nakajima, Y. Honda, O. Kitao, H. Nakai, M. Klene, X. Li, J.E. Knox, H.P. Hratchian, J.B. Cross, C. Adamo, J. Jaramillo, R. Gomperts, R.E. Stratmann, O. Yazyev, A.J. Austin, R. Cammi, C. Pomelli, J.W. Ochterski, P.Y. Ayala, K. Morokuma, G.A. Voth, P. Salvador, J.J. Dannenberg, V.G. Zakrzewski, S. Dapprich, A.D. Daniels, M.C. Strain, O. Farkas, D.K. Malick, A.D. Rabuck, K. Raghavachari, J.B. Foresman, J.V. Ortiz, Q. Cui, A.G. Baboul, S. Clifford, J. Cioslowski, B.B. Stefanov, G. Liu, A. Liashenko, P. Piskorz, I. Komaromi, R.L. Martin, D.J. Fox, T. Keith, M.A. Al-Laham, C.Y. Peng, A. Nanayakkara, M. Challacombe, P.M.W. Gill, B. Johnson, W. Chen, M.W. Wong, C. Gonzalez, J.A. Pople, GAUSSIAN 03, Revision B.03, Gaussian Inc., Pittsburgh PA, 2003.